International Journal of Solids and Structures 50 (2013) 1187–1191

Contents lists available at SciVerse ScienceDirect

International Journal of Solids and Structures

journal homepage: www.elsevier.com/locate/ijsolstr

Phase field simulation of heterogeneous cubic → tetragonal martensite nucleation

Hui She [a], Yulan Liu [a,*], Biao Wang [b]

[a] School of Engineering, Sun Yat-Sen University, 135 Xingang West Road, Guangzhou 510275, China
[b] School of Physics and Engineering, Sun Yat-Sen University, 135 Xingang West Road, Guangzhou 510275, China

ARTICLE INFO

Article history:
Received 8 March 2012
Received in revised form 25 November 2012
Available online 10 January 2013

Keywords:
Heterogeneous martensite nucleation
Phase field model
Microscopic defects
Finite element method

ABSTRACT

The mechanisms for heterogeneous cubic → tetragonal martensite nucleation due to different types of microscopic defects (voids, stress-concentration site, inertial inclusion and pre-existing nucleus) and the temporal evolution of martensite morphology are monitored with finite element simulation of phase filed model. The results demonstrate that the nucleation prefers to occur around void and stress-concentration site initially; high residual stress exists around inertial inclusion; pre-existing nucleus promotes nearby martensite phase to develop on it. The effects of various defects on heterogeneous nucleation are different, and stress relaxation behavior is the dominant factor which characterizes the whole microstructure evolution process.

1. Introduction

Martensitic transformation (MT) is a diffusionless solid-state phase transformation, and can be commonly observed in various metal, alloys and ceramics. Materials undergoing this phase transformation have some special properties, such as steel strengthening and shape-memory effects (Bhattacharya, 2003; Patoor et al., 2006). In order to understand the phenomena and predict the unique properties, the mechanisms of nucleation and the morphology evolution of the martensite phase have become important issues. MT is generally believed to occur by heterogeneous nucleation. Several theories have been proposed to simulate the process. Olson and Cohen (1975) postulated that the intersection of slip bands produced as a result of plastic deformation acts as a nucleation site for martensite. Suzuki et al. (1977) suggested that the local stress concentration near the grain boundaries due to the pile-up of dislocations would aid the martensite nucleation. Clapp (1973) expressed the view that the localized soft mode near a lattice defect may play a key role in the nucleation. In recent years, there is much fundamental research has been done on the theory of MT nucleation (see Olson et al., 1986; Olson and Roytburd, 1995; Reid et al., 1999; Levitas and Javanbakht, 2010). Moreover, much effort has also been made to clarify them experimentally. For example, Zhang et al. (1992) observed by optical microscopy that grain boundary triple junctions and twin boundaries are favorable nucleation sites for thin plate martensite. Saburi and Nenno (1986) found that martensite prefer to nucleate at certain stress concentrations such as dislocation tangles in the matrix, surface steps, boundary dislocation, and metal oxides.

From above, we can conclude the involvement of microscopic defects (such as grain boundary, dislocation and inclusion) may play an important role in martensite nucleation. Due to the rapid dynamics of MT, the different types of heterogeneous martensite nucleation and the specific morphology evolution are still unknown. Till now, numerical simulation methods have become helpful tools for modeling microstructure evolution. For example, Li et al. (2004) investigated the effects of defects on martensite nucleation by molecular dynamics simulation. However this method is restricted by its computation capability. During the past ten years, phase field (PF) model has been extensively studied and been applied to MT (Chen, 2002; Moelans et al., 2008; Yamanaka et al., 2010). In particular, Khachaturyan and co-workers have developed phase-field microelasticity theory, and propose PF model on the basis of the time-dependent Ginzburg–Landau (TDGL) kinetic equations (Khachaturyan, 1983; Wang and Khachaturyan, 1997; Artemev et al., 2001; Ni et al., 2007). Zhang et al. (2007) adopted PF microelasticity model to study heterogeneous MT nucleation triggered in the undercooled parent phase. In their works, the numerical solution to TDGL equations is obtained in the reciprocal space using Fourier transformation.

As we know, a cubic to tetragonal MT involves different variants of martensite. In order to reduce elastic strain energy, domains with a different variant of the tetragonal phase generally interact with each other and arrange in a self-accommodating manner, which is known as self-accommodation MT (Bhattacharya et al., 2004; Wang and Li, 2010). In the present work, a finite element framework of PF model for MT is proposed on the basis of TDGL equations, and it is applied to simulate the heterogeneous cubic → tetragonal martensite nucleation. The influences of different microscopic defects (including voids, stress-concentration sites, inert inclusions and pre-existing martensite nucleus) on

* Corresponding author.
E-mail addresses: stslyl@mail.sysu.edu.cn (Y. Liu), wangbiao@mail.sysu.edu.cn (B. Wang).

0020-7683/$ - see front matter © 2013 Elsevier Ltd. All rights reserved.
http://dx.doi.org/10.1016/j.ijsolstr.2012.12.020

martensite nucleation are investigated. The relaxation progresses for multi-variant martensites are also monitored.

2. Finite element framework for phase field model

Based on diffuse-interface description, PF model describes a microstructure by the evolution of a set of continuum phase-field variables. For the purpose of describing MT, long-range order parameter field $\{\eta_p(\mathbf{r}), p = 1, ..., n\}$ is used to describe spatial phase evolution, where $\mathbf{r}$ is the coordinate vector and n is the number of all possible orientations of martensite variants. The austenite phase under high temperature corresponds to zero order parameters $(\eta_1, ..., \eta_n = 0)$; the pth martensite phase under low temperature is $(\eta_p = 1)$, and narrow interface between the two different phases $(0 < \eta_p < 1)$. The total free energy of the system, F, is defined as

$$F = F_{bulk} + F_{\text{int}} + F_{elast}, \tag{1}$$

where F_{bulk}, F_{int} and F_{elast} denotes the bulk chemical free energy, the interfacial energy and the elastic strain energy, respectively. The bulk chemical energy can be expressed as a conventional Landau polynomial of order parameters, written as

$$F_{bulk} = \int_v \Delta f \left\{ \frac{A}{2}\sum_{p=1}^{n}\eta_p^2 - \frac{B}{3}\sum_{p=1}^{n}\eta_p^3 + \frac{C}{4}\left(\sum_{p=1}^{n}\eta_p^2\right)^2 \right\} dv, \tag{2}$$

where Δf is the transformation driving force that represents the difference between the specific free energies of the martensitic and parent phase; p denotes the pth orientation variant of MTs; A, B and C are the expansion coefficient of the Landau polynomial expansion. The value of A, B and C are chosen to set η as close to either 0 or 1. In the cases of cubic → tetragonal MT, p = 1,2 and 3, corresponding to three orientation variants of the tetragonal phase whose tetragonality axes are along the three ⟨1 0 0⟩ directions in the cubic phase.

The gradient energy, describing non-local effects due to the inhomogeneity of order parameters, is given as

$$F_{\text{int}} = \int_v \left[\sum_{p=1}^{n} \frac{1}{2}\beta_{ij}(p)\frac{\partial \eta_p}{\partial x_i}\frac{\partial \eta_p}{\partial x_j} \right] dv, \tag{3}$$

where $\beta_{ij}(p)$ is the positively defined gradient energy coefficient tensors.

The elastic strain energy is derived as a coupled function of strain and order parameter (Khachaturyan, 1983):

$$F_{elast} = \int_v \frac{1}{2} C_{ijkl}\varepsilon_{ij}^{el}\varepsilon_{kl}^{el} dv, \tag{4}$$

where C_{ijkl} is the elastic coefficient matrix; and the elastic strain tensor ε^{el} is define as a deviation of the total strain ε from the stress free strain (eigen strain) ε^0, i.e.,

$$\varepsilon_{ij}^{el} = \varepsilon_{ij} - \varepsilon_{ij}^{0}. \tag{5}$$

The total strain ε conform to the usual geometric equation

$$\varepsilon_{ij} = \frac{1}{2}\left(\frac{\partial u_k}{\partial x_i} + \frac{\partial u_k}{\partial x_j}\right). \tag{6}$$

For proper MTs, the total stress-free stain ε^0 is related to order parameter as

$$\varepsilon_{ij}^{0} = \sum_{p=1}^{n} \eta_p \varepsilon_{ij}^{00}(p), \tag{7}$$

where $\varepsilon_{ij}^{00}(p)$ is the pth transformation-induced eigen strain. For the cubic → tetragonal transformation, the pth variants of $\varepsilon_{ij}^{00}(p)$ are given by the following matrices:

$$\varepsilon_{ij}^{00}(1) = \begin{bmatrix} \varepsilon_3 & 0 & 0 \\ 0 & \varepsilon_1 & 0 \\ 0 & 0 & \varepsilon_1 \end{bmatrix}, \tag{8}$$

$$\varepsilon_{ij}^{00}(2) = \begin{bmatrix} \varepsilon_1 & 0 & 0 \\ 0 & \varepsilon_3 & 0 \\ 0 & 0 & \varepsilon_1 \end{bmatrix}, \tag{9}$$

$$\varepsilon_{ij}^{00}(3) = \begin{bmatrix} \varepsilon_1 & 0 & 0 \\ 0 & \varepsilon_1 & 0 \\ 0 & 0 & \varepsilon_3 \end{bmatrix}, \tag{10}$$

Here the components of these matrices are $\varepsilon_1 = (a_t - a_c)/a_c$ and $\varepsilon_3 = (c_t - a_c)/a_c$, where a_t, c_t and a_c are the crystal lattice parameters along the a and c axes of the tetragonal phase and that along a axis of the cubic phase, respectively.

The evolution of phase field is governed by TDGL kinetic equations. The obtained linear dependence of the rate on the transformation driving force is the TDGL equations. That is

$$\frac{\partial \eta_p(\mathbf{r}, t)}{\partial t} = -\hat{L}_{pq}\frac{\delta F}{\delta \eta_q}, \tag{11}$$

where $\hat{L}_{pq}$ is the matrix of kinetic coefficients. The variation of the functional free energy F is given as

$$\delta F = \delta F_{bulk} + \delta F_{\text{int}} + \delta F_{elast}, \tag{12}$$

where

$$\delta F_{bulk} = \int_v \Delta f \sum_{q=1}^{n}\left[A\eta_q - B\eta_q^2 + C\eta_q\left(\sum_{q=1}^{n}\eta_q^2\right)\right]\delta\eta_q dv, \tag{13a}$$

$$\delta F_{\text{int}} = -\int_v \sum_{q=1}^{n}\beta_{ij}\frac{\partial^2 \eta_q}{\partial x_i \partial x_j}\delta\eta_q dv + \int_v \frac{\partial}{\partial x_j}\left(\sum_{q=1}^{n}\beta_{ij}\frac{\partial \eta_q}{\partial x_i}\delta\eta_q\right) dv, \tag{13b}$$

$$\delta F_{elast} = \int_v C_{ijkl}\varepsilon_{ij}^{el}\delta\varepsilon_{kl} dv - \int_v C_{ijkl}\varepsilon_{ij}^{el}\sum_{q=1}^{n}\varepsilon_{kl}^{00}(q)\delta\eta_q dv. \tag{13c}$$

Substituting Eqs. (12, 13a–c) into Eq. (11) results in

$$\frac{\partial \eta_p}{\partial t} = \hat{L}_{pq}\sum\nolimits_{q=1}^{n}\left\{ \beta_{ij}\frac{\partial^2 \eta_q}{\partial x_i \partial x_j} - \underline{\Delta f\left[A\eta_q - B\eta_q^2 + C\eta_q\left(\sum_{q=1}^{n}\eta_q^2\right)\right] + \sigma_{ij}\varepsilon_{ij}^{00}(q)}\right\}, \tag{14}$$

where the stress $\sigma_{ij} = C_{ijkl}\varepsilon_{kl}^{el}$. This equation resembles the heat transfer equation and the underlined part can be treated as the heat source. The analogy was suggested by Levitas et al., and the finite element solutions are presented in their works (Levitas and Lee, 2007; Levitas et al., 2009, 2010). When material tensors are isotropic, we have $\beta_{ij} = \beta\delta_{ij}$ and $\hat{L}_{pq} = \hat{L}\delta_{pq}$, where δ is the Kronecker delta.

The thermo-mechanical equilibrium equations and boundary conditions are identical with conventional ones and are abbreviated in this paper. Till now, a system of coupled thermoelasticity and heat transfer problem is constructed. A finite element formulation can be developed by applying the isoparametric interpolations for node displacement and order parameters. The algorithm is implemented into the finite element software "Comsol".

3. Numerical simulation

A two-dimensional plane-strain simulation of cubic → tetragonal MT in a square domain with dimensions of 50 nm × 50 nm is considered. An ellipsoidal heterogeneous site (aspect ratio of semi axis $a : c = 5 : 1$, a = 5 nm) is located at the center of the austenitic domain (shown in Fig. 1). The angle between the orientation of one

axis of the ellipsoid and the x-axis of the Cartesian coordinate system is 45°. The following material parameters are used (Idesman et al., 2008): Young's modulus $E = 198\ 300$ MPa; Poisson's ratio $v = 0.33$; density $\rho = 5850\ \mathrm{kg/m^3}$; the isotropic gradient energy coefficient $\beta = 2.33 \times 10^{-10}$ N; the isotropic kinetic parameter of the TDGL equation $\hat{L} = 2596.5\ \mathrm{m^2/N\ s}$; the chemical driving force $\Delta f = 10^9\ \mathrm{J/m^3}$; the expansion coefficient of the Landau polynomial expansion $A = 0.14$, $B = 12.42$, $C = 12.28$; the variants of the transformation-induced eigen strain are given by $\varepsilon_{ij}^{00}(1) = \begin{bmatrix} 0.1 & 0 \\ 0 & -0.1 \end{bmatrix}$ and $\varepsilon_{ij}^{00}(2) = \begin{bmatrix} -0.1 & 0 \\ 0 & 0.1 \end{bmatrix}$.

The initial conditions are as follows: the initial random distribution of the order parameters η_1 and η_2 with values between 0 and 1 is given. The whole boundary are prescribed as zero thermo fluxes ($\frac{\partial \eta}{\partial n} = 0$, n ψ is the outward normal to the boundary). The observation time $t = 6 \times 10^{-10}$ s is subdivided into 300 time steps with a time increment $\Delta t = 2 \times 10^{-12}$ s. Need to mention, all the final morphologies below refer to the solution at the end of the observation time.

4. Results and discussions

To gain a basic understanding of the effects of microscopic defects on the evolution of MT heterogeneous nucleation, we assume the ellipsoidal site as a void, stress-concentration site, inert inclusion and pre-existing nucleus, respectively. For comparison, the morphologies of homogenous nucleation are simulated firstly.

4.1. Homogenous nucleation

Here an ideal nucleation in a homogenous system is simulated (Levitas and Lee, 2007; Levitas et al., 2010). The martensite morphologies of variant 1 at the initial, the intermediate and the final stage are shown in Fig. 2(a–c) respectively, where the red domains represent martensite phases of variant 1 ($\eta_1 = 1$), the blue domains represent austenite or martensite phases of variant 2 ($\eta_1 = 0$), and the domains with other colors represent the transitional phase from austenite to martensite phase ($0 < \eta_1 < 1$). We notice that the initial randomly distributed order parameters converge to either 0 or 1 finally and correspond to a well-organized microstructure. Fig. 2(d) shows the final morphology of variant 2, where the red domains represent martensite phases of variant 2 ($\eta_2 = 1$) and the blue domains represent austenite or martensite phases of variant 1 ($\eta_2 = 0$). Comparing figures (c) and (d), we can see that interfaces separate two sets of fine twins and a self-accommodated twinned microstructure is constructed. The twin structure of variant 1 and 2 is the result of energy minimization.

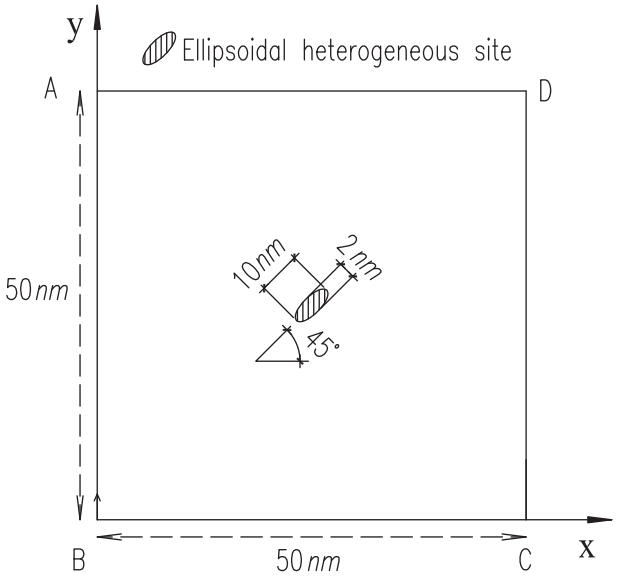

Fig. 1. An austenitic domain with an ellipsoidal heterogeneous site at the center.

4.2. Void

Assume the ellipsoidal site as a void (Levitas et al., 2009). The simulated nucleation and the final martensite phases of variant 1 are shown in Fig. 3(a) and (b), those of variant 2 are shown in (c and d) respectively. What the colors represent are the same with above. From figures (a) and (c), we can see that the initial favorable nucleation sites locate at the endpoints of the major axis of ellipsoid. As we know, MTs are driven by the decrease of the bulk-chemical free energy from austenite to martensite phase but at the cost of increased bulk elastic energy and the gradient energy at the interface. Because void or free surface is in favor of elastic strain energy release, it lowers down the energy barrier of the transformation. So the nucleation chooses to occur at the easiest points. In the following process, stress relaxation is mainly achieved by phase grow-up and coalescence. From figures (b) and (d), we can also see that, due to the interference of the void, the symmetry of the final morphology is broken.

4.3. Stress-concentration site

Grain boundary junction or dislocation may cause local stress concentration. In this case, the influence of stress concentration on nucleation is investigated. Assume the central ellipsoid site is under a uniform tensile stress $p = 1 \times 10^9\ \mathrm{N/m^2}$. Fig. 4 (a) and (b) illustrate the nucleation and the final martensite morphologies of variant 1 respectively, while (c) and (d) are of variant 2. From (a) and (c), we can see that nucleation happens along the major axis of the ellipsoid initially. According to the analysis of stress distribution, the maximum stress values locate there, that proves nucleation also preferentially happens at stress concentration sites. The stress field may stimulate MT of one variant and hinder MT of the other variant depending on whether it is in favor of relaxation of the transformation-induced stress or not. We can infer from (b) and (d), the tensile stress is in favor of MT of variant 1, because the volume fractions of martensitic phase 1 is obviously higher than that of variant 2. If we change tensile stress into compressive stress $p = -1 \times 10^9\ \mathrm{N/m^2}$, all the pictures are on the contrary, i.e., pictures (a and b) are of variant 2 and (c and d) are of variant 1. Besides, the final microstructure merges into two part and is separated into martensite phase of variant 1 and 2 by one interface. That shows the external stress also helps the phase coalesce to eliminate the interfaces, and therefore relaxes the bulk strain energy and the gradient energy at the interfaces.

4.4. Inert inclusion

Impurities are commonly observed in metal and alloys. We consider the ellipsoid site as an inertial inclusion, which means it is incapable of phase transformation. Fig. 5(a) and (b) show the nucleation and the final martensite morphologies of variant 1 respectively, while (c) and (d) are of variant 2. At first stage, no obvious favorable nucleation sites are observed in figures (a) and (c). The twin structure of martensite variant 1 and 2 are rather uniformly distributed and surround the inert inclusion. Along with the relaxation progress, the inclusion begins to constrain the development of the martensite phases, stress concentration occurs around the ellipsoid. In order to reduce the strain energy, the defect is totally trapped in the martensite phase of variant 2, as shown in figures (b) and (d). It can be concluded that the embedded inclusion may bring in high residual stress around it in the process

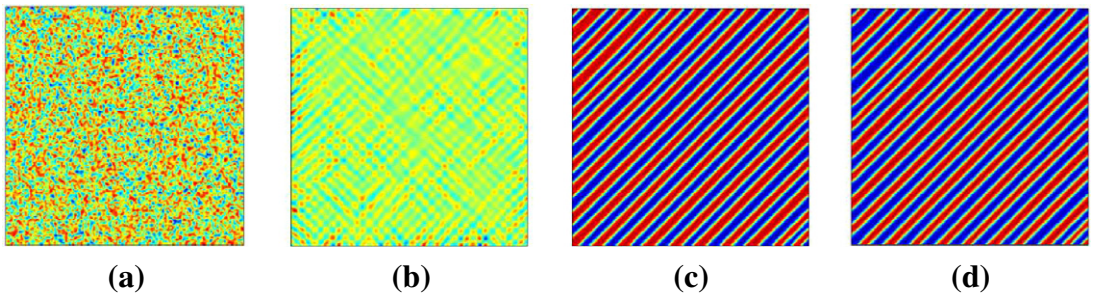

Fig. 2. Evolution of the homogenous martensitic nucleation. Pictures (a–c) are the initial, the intermediate and the final martensite morphologies of variant 1, respectively. Picture (d) is the final morphology of variant 2.

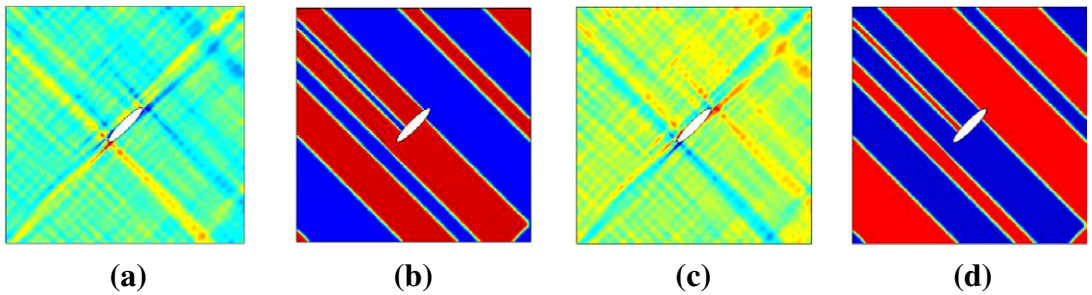

Fig. 3. Evolution of the heterogeneous martensitic phase with an ellipsoid void at the center. Pictures (a and b) correspond to the nucleation and the final martensite morphologies of variant 1 respectively, and (c and d) are of variant 2.

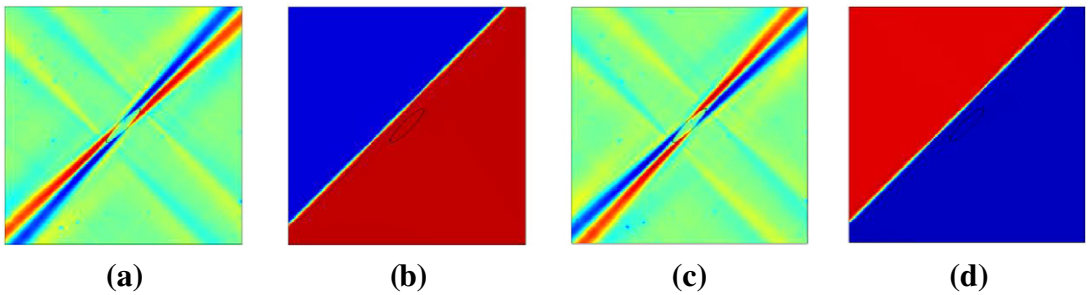

Fig. 4. Evolution of the heterogeneous martensitic phase with an central ellipsoid site under tensile stress. Pictures (a and b) correspond to the nucleation and the final martensite morphologies of variant 1 respectively, and (c and d) are of variant 2.

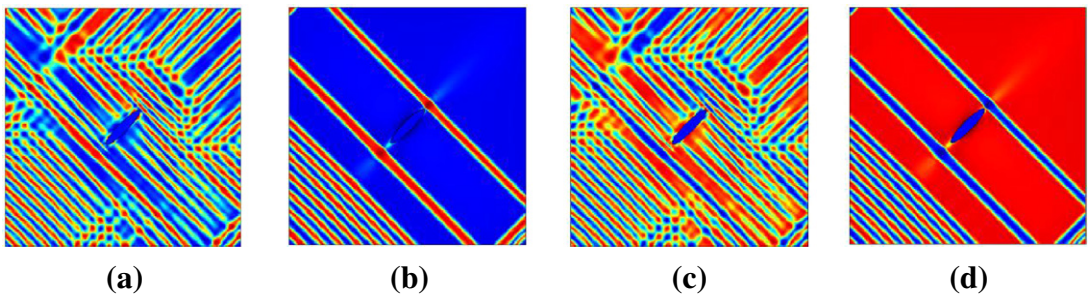

Fig. 5. Evolution of the heterogeneous martensitic phase with an ellipsoid inert inclusion at the center. Pictures (a and b) correspond to the nucleation and the final martensite morphologies of variant 1 respectively, and (c and d) are of variant 2.

of MT, which shall be harmful to the whole martensite mechanical properties.

4.5. Pre-existing nucleus

Finally, let us consider an ellipsoidal pre-existing nucleus at the center of the austenite domain (Levitas and Javanbakht, 2010). The initial conditions are zero order parameters, $\eta_1 = \eta_2 = 0$, for the whole specimen except the initial martensitic embryo located, where intermediate values of the order parameters ($\eta_1 = \eta_2 = 0.5$) are given. Fig. 6(a) and (b) shows the nucleation and the final martensite morphologies of variant 1 respectively, while (c) and (d) are of variant 2. Figures (a) and (c) show that follow-up martensite phase grows on the pre-existing nucleus. If we tune

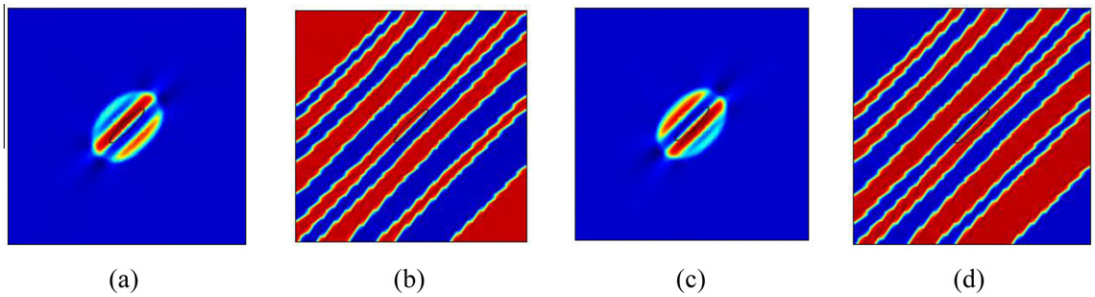

Fig. 6. Evolution of the heterogeneous martensitic phase with an ellipsoidal pre-existing nucleus at the center. Pictures (a and b) correspond to the nucleation and the final martensite morphologies of variant 1 respectively, and (c and d) are of variant 2.

the shape or orientation of the embryo, the martensite phase will adjust to grow on it accordingly. The nucleus is a driving source of the phase transformation, and plays a key role on the evolution of martensite phase. An initial nucleus can stimulate and influence nearby MT to develop on it. That is identical with experiments observation, i.e., MT develop at a rapid rate once initial nucleation forms.

5. Conclusions

In this paper, a finite element framework of PF model for MT is proposed on the basis of TDGL equations, and it is applied to investigate the relationship of the heterogeneous nucleation with microscopic defects (including void, stress-concentration site, inert inclusion and pre-existing martensite nucleus). Numerical results show, in the absence of any defects, homogenous cubic to tetragonal MT usually arrange themselves in a fine structure of twining phases. Under influence of various defects, nucleation choose an optimum path to reduce the system free energy. Nucleation prefers to occur around void and stress-concentration site. Void lows down the energy barrier of MT because elastic strain energy can be released around it. Stress concentration may stimulate MT of one variant but hinder MT of the other variant depending on it is in favor of stress relaxation of transformation-induced strain or not. Besides, external stress also helps coalescence of martensite phase. The embedded inertial inclusion constrains MT and brings in high residual stress around it. Pre-existing nucleus can promote nearby martensite phase to develop on it.

To be concluded, microstructure evolution is to reduce the system free energy, and stress relaxation behavior is the dominant factor which characterizes the whole microstructure evolution process. Understanding the mechanisms of various heterogeneous nucleation may help us to design a specific purposed martensite microstructure.

Acknowledgements

This project is grateful for support from the National Natural Science Foundation of China (Nos. 10902128, 10732100, 50802026, 10972239, 11072271), the Fundamental Research Funds for the Central Universities. Hui She wishes to thank Dr. Wang Gang for instructions and helps on COMSOL.

References

Artemev, A., Jin, Y., Khachaturyan, A.G., 2001. Three-dimensional phase field model of proper martensitic transformation. Acta Materialia 49, 1165–1177.

Bhattacharya, K., 2003. Why It Forms and How It Gives Rise to the Shape-Memory Effect. Oxford Univ. Press.

Bhattacharya, K., Conti, S., Zanzotto, G., Zimmer, J., 2004. Crystal symmetry and the reversibility of martensitic transformations. Nature 428, 55–59.

Chen, L.-Q., 2002. Phase-field models for microstructure evolution. Annual Review of Materials Research 32, 113–140.

Clapp, P.C., 1973. A localized soft mode theory for martensitic transformations. Physica Status Solidi (b) 57, 561–569.

Khachaturyan, A.G., 1983. Theory of Structural Transformation in Solids. Wiley-Interscience Publications.

Idesman, A.V., Cho, J.-Y., Levitas, V.I., 2008. Finite element modeling of dynamics of martensitic phase transitions. Applied Physics Letter 93, 043102.

Levitas, V.I., Javanbakht, M., 2010. Surface tension and energy in multivariant martensitic transformations: phase-field theory, simulations, and model of coherent interface. Physical Review Letters 105, 165701.

Levitas, V.I., Lee, D.-W., 2007. A thermal resistance to interface motion in the phase-field theory of microstructure evolution. Physical Review Letters 99, 245701.

Levitas, V.I., Lee, D.-W., Preston, D.L., 2010. Interface propagation and microstructure evolution in phase field models of stress-induced martensitic phase transformations. International Journal of Plasticity 26, 395–422.

Levitas, V.I., Levin, V.A., Zingerman, K.M., Freiman, E.I., 2009. Displacive phase transitions at large strains: phase-field theory and simulations. Physical Review Letters 103, 025702.

Li, B., Zhang, X.M., Clapp, P.C., Rifkin, J.A., 2004. Molecular dynamics simulations of the effects of defects on martensite nucleation. Journal of Applied Physics 95, 1698–1705.

Moelans, N., Blanpain, B., Wollants, P., 2008. An introduction to phase-field modeling of microstructure evolution. Calphad 32, 268–294.

Ni, Y., Jin, Y.M., Khachaturyan, A.G., 2007. The transformation sequences in the cubic → tetragonal decomposition. Acta Materialia 55, 4903–4914.

Olson, G., Cohen, M., 1975. Kinetics of strain-induce martensitic nucleation. Metallurgical Transactions A 6, 791–795.

Olson, G.B., Cohen, M., 1986. Dislocation theory of martensitic transformations. In: Nabarro, F.R.N. (Ed.), Dislocations in Solids, 7. Elsevier Science Publishers B V, pp. 297–407.

Olson, G.B., Roytburd, A.L., 1995. Martensitic nucleation. In: Olson, G.B., Owen, W.S. (Eds.), Martensite, 9. The Materials Information Society, pp. 149–174.

Patoor, E., Lagoudas, D.C., Entchev, P.B., Brinson, L.C., Gao, X., 2006. Shape memory alloys. Part I: General properties and modeling of single crystals. Mechanics of Materials 38, 391–429.

Reid, A.C.E., Olson, G.B., Moran, B., 1999. Dislocations in nonlinear nonlocal media: martensitic embryo formation. Phase Transitions 69, 309–328.

Saburi, T., Nenno, S. 1986. In: Proc. of ICOMAT-86, The Japan Institute of Metals, pp. 671–678.

Suzuki, T., Kojima, H., Suzuki, K., Hashimoto, T., Ichihara, M., 1977. An experimental study of the martensite nucleation and growth in 18/8 stainless steel. Acta Metallurgica 25, 1151–1162.

Wang, Y., Khachaturyan, A.G., 1997. Three-dimensional field model and computer modeling of martensitic transformations. Acta Materialia 45, 759–773.

Wang, Y., Li, J., 2010. Phase field modeling of defects and deformation. Acta Materialia 58, 1212–1235.

Yamanaka, A., Takaki, T., Tomita, Y., 2010. Elastoplastic phase-field simulation of martensitic transformation with plastic deformation in polycrystal. International Journal of Mechanical Sciences 52, 245–250.

Zhang, W., Jin, Y.M., Khachaturyan, A.G., 2007. Phase field microelasticity modeling of heterogeneous nucleation and growth in martensitic alloys. Acta Materialia 55, 565–574.

Zhang, X.M., Li, D.F., Zhao, S., Xing, Z.S., Zhang, J.Z., Gantier, E., Simon, A. 1992. In: Proc. of ICOMAT-92, Monterey, California, USA, pp. 493–497.